SPE
Society of Petroleum Engineers of AIME

SPE 6858

THE MORPHOLOGY OF DISPERSED CLAY IN SANDSTONE RESERVOIRS AND ITS EFFECT ON SANDSTONE SHALINESS, PORE SPACE AND FLUID FLOW PROPERTIES

by John W. Neasham, Shell Development Company

ABSTRACT

Three categories of dispersed clay are described for hydrocarbon-bearing sandstones using scanning electron microscopy and correlated to rock geological-petrophysical parameters commonly used in reservoir evaluation. Dispersed clays can occur in pores as (a) discrete (not intergrown) particles, (b) intergrown crystal linings on pore walls, and (c) crystals bridging across pores. These different clay morphologies significantly affect sandstone porosity/permeability, capillary pressure curve and associated pore-size distribution parameters, and "shaliness" indicators from X-ray diffraction and Q_v measurements.

INTRODUCTION

The increased utilization of scanning electron microscopy (SEM) and associated elemental detection systems (e.g., energy dispersive analysis of X-rays) has greatly expanded our knowledge of dispersed clay morphology and mode of occurrence in sandstone reservoir rocks. The marginal or questionably productive nature of particular hydrocarbon-bearing zones can be due to silicate clay crystals developed within rock pores in a manner adversely affecting fluid flow. Variations in clay crystal morphology can change a hydrocarbon zone from economically nonproductive to productive, and vice versa. In the past, the direct observation and description of this important rock property was limited to petrographic microscope techniques. Recent technological advances in SEM, however, have enabled the petroleum geologist routinely to study rock mineral, textural, and pore-space properties at magnifications, resolution, and depth of focus far exceeding petrographic thin section capabilities.

Several recent papers have described and discussed the importance of dispersed clays in sandstones.[1-3] This paper defines "dispersed" clay as silicate clay minerals (e.g., kaolinite, illite, smectite, chlorite) developed within the rock pore system and generally attached to rock mineral surfaces. Dispersed clay in rocks is of diagenetic (i.e., authigenic) origin, having developed subsequent to sediment deposition by precipitation of clay crystals from pore fluids. Particular clay mineral species develop in response to changes in pore water chemistry brought about by changing temperature, pressure and groundwater conditions during burial and compaction. Since dispersed clays generally occur as a rock pore-filling component and have a variety of crystal sizes and shapes, they exhibit a broad spectrum of adverse effects on rock fluid flow and fluid saturation properties.

References and illustrations at end of paper.

This paper describes (a) three basic types of dispersed clay in sandstones and (b) several laboratory measured geological-petrophysical properties associated with each of these three clay types that are commonly used in evaluating hydrocarbon-bearing reservoirs. Specifically, 14 sandstone samples are classified into three general categories on the basis of dispersed clay morphology as revealed by SEM. Each category is characterized by the following rock petrophysical parameters: porosity and air permeability, oil and water relative permeability, air/mercury capillary pressure curves, pore size and sorting, cation exchange capacity, and the amount of pore-filling clay estimated from X-ray diffraction and thin section analysis.

DISPERSED CLAY CATEGORIES

The basic criteria used to define and contrast the three general types of dispersed clay in sandstones are (a) clay crystal structure and (b) location on pore walls (i.e., mineral surfaces) and/or within intergranular pores and pore throats. Since the primary objective of this paper is to set forth the relationship of dispersed clay types to sandstone petrophysical properties, detailed discussions of specific clay types and morphologies are not presented. The aforementioned Refs. 1 through 3 can be referred to for this information.

The three categories of dispersed clay are as follows.

1. Discrete particle clays reflect the typical

mode of occurrence of kaolinite in sandstones. It usually develops as pseudohexagonal, platy crystals attached as discrete particles to pore walls or occupying intergranular pores (Fig. 1A). The crystal platelets may be stacked face-to-face forming long crystal aggregates (i.e., vermicular or "booklike" kaolinite). Kaolinite crystals of either a singular or stacked platelet morphology are characteristically scattered ("patchy") throughout the pore system and do not form intergrown crystal frameworks on pore walls or within intergranular pores. Kaolinite crystals that extensively fill pores have a random arrangement with respect to one another and affect rock petrophysical properties primarily by (a) reducing intergranular pore volume and (b) behaving as migrating "fines" in the pore system.

2. Pore-lining clays are attached to pore walls to form a relatively continuous and thin (≤ 12 microns) clay mineral coating (Fig. 1B). The clay crystals may be oriented either parallel or perpendicular to the pore wall surface. Crystals attached perpendicular to the pore wall surface are usually intergrown to form a continuous clay layer containing abundant micropore space, with pore diameters in the 2-micron to submicron range. Illite, chlorite, and montmorillonite clays have been observed with pore-lining crystal morphologies.

3. Pore-bridging clays also include illite, chlorite, and montmorillonite varieties that, in addition to being attached to pore wall surfaces, extend far into or completely across a pore or pore throat to create a bridging effect (Fig. 1C). SEM photomicrographs of sandstones containing pore-bridging clays show the extensive development of intergrown and/or intertwined clay crystals within the pore system, creating both microporosity and tortuous fluid flow pathways.

RELATION OF DISPERSED CLAY TYPES TO SANDSTONE GEOLOGICAL AND PETROPHYSICAL PROPERTIES

The suite of 14 sandstone samples used to illustrate selected dispersed clay/geological/petrophysical relationships are listed by their formation name on Tables 1 and 2. These sands cover a porosity (at 1,000 psig) and air permeability (unstressed and klinkenberg corrected) range of 8.45 to 26.5 percent and 0.09 to 1,173 md, respectively. Criteria used to select these samples, which were drawn from a larger sample population of 44 hydrocarbon-producing sandstones, were (a) they have similar textural properties (basically fine to very fine grain size and well to very well sorting - Fig. 2); (b) they have dissimilar types of dispersed clays within their pore system; and (c) dispersed clays are the dominant pore-filling component affecting the rock's geological and petrophysical properties. The comparison of sandstone samples of similar texture was a necessary requirement for this study, since texture alone is of first-order importance in affecting rock pore size and, hence, fluid flow properties. Elimination of texture as a significant variable among the 14 sand samples permitted a direct comparison of reservoir parameters with differences in the pore-filling dispersed clay component of rock samples.

The following geological and petrophysical properties commonly used in the evaluation of reservoir rock quality and productivity potential are correlated to dispersed clay properties.

1. Porosity/Air Permeability - The subdivision of sandstone dispersed clay morphology into particle, lining, and bridging categories is strongly reflected by sample porosity/air permeability correlations (Fig. 3). The clay morphology of the highest air permeability sands is predominantly the discrete particle (not intergrown) type. SEM data for this sand type shows the following pore space (and pore wall) characteristics: (a) an abundance of clean (no clay) original sand grain surfaces or secondary, silica overgrowth crystal surfaces, and (b) vermicular kaolinite crystals scattered over and attached to grain surfaces and/or filling intergranular pore space as a patchy clay crystal aggregate (Fig. 4). A relatively high permeability-to-porosity relationship characterizes these sands because the morphology and distribution of the dispersed clay does not significantly restrict air flow through pores and pore throats.

Dispersed clay morphology for samples in the intermediate air permeability range on Fig. 3 is predominantly of a pore-lining variety. SEM photomicrographs for this sand category show pore walls extensively coated with clay crystals (e.g., chlorite and/or illite), yet the intergranular pores remain relatively open (free of clay) (Fig. 5). Hence, sands with pore-lining clays can have both significant amounts of clay and relatively good air flow properties.

The low-permeability sandstones on Fig. 3 contain pore-bridging clay types. SEM data for these samples show a clay morphology characterized by (a) intergrown crystal platelets (e.g., chlorite) attached to sand grain surfaces and bridging across intergranular pore space, and (b) fibrous, intergrown crystals (e.g., illite) extending far into and/or across intergranular pores (Fig. 6). This bridging clay morphology forms partial to complete barriers to fluid flow and can seriously impair rock permeability, even for sands of relatively high porosity and low clay content.

2. Pore-size Distribution - The rock properties of median pore diameter (M_{dp}) and pore sorting coefficient (S_{op}) can be calculated from a pore-size distribution curve. Such a curve is similar to a grain-size distribution curve except it represents the cumulative volume (percent) of pores bounded by pore necks larger than a given size. The M_{dp} and S_{op} parameters, which are obtained from capillary pressure curve and initial-residual saturation data, are distinctly different for the three sandstone groups (Table 1). The discrete particle through pore-lining to pore-bridging categories show a declining average median pore-diameter values of 24.2 through 6.0 to 0.94 microns, respectively. Pore size sorting becomes progressively worse, with corresponding values of 1.14 (very well) through 1.56 (moderate) to approximately 2.24 (poorly sorted). Pore-size distribution parameters for the discrete particle samples are strongly related to grain-size distribution parameters (median grain size and sorting). In other words, the grain-size distribution controls the pore-size distribution that, in turn, affects the rock's permeability for this rock type. For the pore-lining and pore-bridging categories, however, the influence of grain-size distribution on pore-size distribution is minimal. Reference to Table 1 shows that, although the lining and bridging categories average a fine grain size and

well sorting, they have much smaller and more poorly sorted pore sizes. These data reflect the progressively detrimental effect of pore-lining and pore-bridging clay morphologies on effective pore throat diameters and, hence, rock permeability. The 1-micron median pore diameter for sands containing pore-bridging clay is evidence that the effective pores and pore throat diameters are developed within the intergrown dispersed clay crystals rather than between the sand grains.

3. Air-Mercury Capillary Pressure Curves - The three clay-containing sandstone categories show basic differences in capillary pressure curves (Fig. 7 and Table 1) that are indicative of their respective pore network properties. These capillary pressure-curve differences are reflected by their respective Thomeer parameters,[4] which mathematically express both the location (extrapolated initial mercury/air injection pressure, or P_d) and shape (pore geometrical factor, or G) of the curve. Comparison of average Thomeer parameter values for the three categories show the following relationships: (a) sands in the discrete particle group have low pore geometrical factors ($\bar{G}$ = 0.10) and initial mercury injection (displacement) pressures ($\bar{P}_d$ = 7.1 psia); (b) sands with a pore-lining clay morphology show higher, more complex pore geometrical factors ($\bar{G}$ = 0.55), and injection pressures ($\bar{P}_d$ = 22.2 psia); (c) the pore-bridging samples have high mercury injection pressures ($\bar{P}_d$ = 82.8 psia). Pore geometrical factor values for the bridging category are considered to be nonrepresentative due to the combined effect of high pore entry pressures and the inability to obtain a full curve because the upper curve data point are limited to 1,000 psia.

4. Relative Permeability - End-point oil relative permeability values are around 1.0 (± 0.1) for all three sand categories, even though the more shaly pore-lining and pore-bridging categories have generally higher connate water saturations than the discrete particle samples (Table 2). This k_{ro} value of approximately 1.0 holds because the end-point connate (immobile) water saturation during oil flow (k_o at S_{wc}) is held (wets) in the finer-pore system rather than the larger pores, which are the chief contributors to measured fluid flow. It is also noted that the two oil-wet sand samples on Table 2 have much lower k_{ro} values (0.67 and 0.20) and lower immobile water saturations. These two samples reflect increased trapping of the nonwetting phase (water) within larger pores and at pore throats. The end-point brine relative permeability values (Table 2) show a progressive decline (0.14 - 0.10 - 0.05) for the discrete particle, pore-lining, and pore-bridging categories, respectively. This declining k_{rw} appears to be due to greater constrictions to brine flow in the progressively finer-pore systems as the immobile oil (nonwetting phase) is trapped within larger pores and at their pore throats.

5. Clay Mineral Content - The clay content of a sandstone sample can be expressed as (a) type and amount of clay minerals from X-ray diffraction, (b) petrographic analysis data from thin sections, and (c) cation exchange capacity (MEQ/100 grams of sample) and/or Q_v values[5] (MEQ/ml pore volume). Clay mineral content from X-ray is semi-quantitative at best and includes both diagenetic and detrital (e.g., mica, glauconite, and/or argillaceous grains) varieties. The percent-clay value on Table 1, therefore, is an estimate of the amount of pore-filling (i.e., diagenetic) clay based on both X-ray data and pore-filling clay observed in thin section.

The discrete particle group of sands have a relatively low clay content (~5 percent) and Q_v (0.03). Hence, this sand type is generally classified as a clean sand. The pore-lining and pore-bridging categories contain significantly greater amounts (and types) of clay minerals (7 to 20 percent) and higher Q_v values (0.11 to 0.69; slightly shaly to very shaly). The similar amounts of clay and Q_v values for the pore-lining and pore-bridging categories do not reflect their aforementioned differences in porosity/permeability, pore-size distribution, and capillary pressure-curve properties. Only when the dispersed clay morphology as revealed by SEM analysis is documented do the sand samples segregate into two distinct groupings of reservoir quality rock.

CONCLUSIONS

This paper documents the strong influence of commonly occurring dispersed clay minerals on sandstone porosity/permeability correlations, pore size parameters, capillary pressure curves, oil-water relative permeability, and shaliness indicators. These relationships have been applied to samples of similar textural properties in order to demonstrate the relative effect of discrete particle, pore-lining, and pore-bridging clay types on sandstone petrophysical parameters. It must be recognized that significant differences in textural properties also can exert a strong control on rock pore space and permeability, and rocks in the moderate and poorly sorted categories must be evaluated on the basis of both texture and clay morphology. In either case, SEM analysis of a rock sample and description of its clay mineral components can provide valuable information on reservoir productivity potential.

REFERENCES

1. Neasham, J. W.: "Applications of Scanning Electron Microscopy to the Characterization of Hydrocarbon-Bearing Rocks," Scanning Electron Microscopy (March 1977) I, 101-108.
2. Wilson, M. D. and Pittman, E. D.: "Authigenic Clays in Sandstones: Recognition and Influence on Reservoir Properties and Paleoenvironmental Analysis," J. Sed. Petrol. (March 1977) 47, No. 1, 3-31.
3. Almon, W. R. and Davies, D. K.: "Understanding Diagenetic Zones Vital," Oil and Gas J. (June 6, 1977) 209-216.
4. Thomeer, J. H. M.: "Introduction of a Pore Geometrical Factor Defined by the Capillary Pressure Curve," J. Pet. Tech. (March 1960) 73-77.
5. Waxman, M. H. and Smits, L. J. M.: "Electrical Conductivity in Oil Bearing Shaly Sands," Soc. Pet. Eng. J. (June 1968) 107-122.
6. Klinkenberg, L. J.: "The Permeability of Porous Media to Liquids and Gases," Drill. and Prod. Prac., API (1941) 200.

Table 1

GEOLOGICAL AND PETROPHYSICAL PROPERTIES OF SELECTED SANDSTONE SAMPLES

Sample Formation Name	Pore Size and Sorting[1]		Grain Size and Sorting[2]		Thomeer Parameters[3]		Clay Content[4]		
	$M_{dp}(\mu)$	S_{op}	$M_d(\mu)$	S_o	G	P_d	% Clay	Q_v	Degree of "Shaliness"
"Discrete Particle" Clays (see Fig. 1A)									
Berea	25.7	1.17	170	1.17	0.12	6.5	5	0.03	clean
Miocene "S"	31.0	1.09	145	1.14	0.04	6.2	5	0.03	clean
Paluxy	23.8	1.02	110	1.25	0.05	7.8	5	0.02	clean
Cotton Valley	21.2	1.27	166	1.36	0.15	6.8	6	0.06	clean
Tar Springs	19.2	1.13	146	1.25	0.14	8.2	3	0.03	clean
Average Values	24.2	1.14	146	1.23	0.10	7.1	5	0.03	clean
"Pore-Lining" Clays (see Fig. 1B)									
Tuscaloosa	10.9	1.38	180	1.34	0.70	8.8	15	0.11	sl. shaly
Vicksburg	5.6	1.69	253	1.41	0.80	14.5	11	0.14	sl. shaly
Hosston	2.2	1.37	235	1.40	0.50	50.0	7	0.13	sl. shaly
Wilcox	3.5	2.14	245	1.41	0.50	20.5	10	0.37	shaly
Frio	8.0	1.23	88	1.20	0.25	17.1	12	0.36	shaly
Average Values	6.0	1.56	200	1.36	0.55	22.2	11	0.22	mod. shaly
"Pore-Bridging" Clays (see Fig. 1C)									
Vicksburg	0.54	2.37	162	1.31	2.50	47.0	20	0.15	sl. shaly
Hosston	1.34	1.28	253	1.44	0.35	92.0	10	0.20	mod. shaly
Wilcox	0.42	2.50	113	1.20	.30	122.0	10	0.54	v. shaly
Wilcox	1.47	2.82	71	1.41	.20	70.0	10	0.36	shaly
Average Values	0.94	2.24	150	1.36	--	82.8	12	0.31	shaly

1) "M_{dp}" is median pore throat diameter; S_{op} is a measure of pore sorting.
2) Textural parameters from "wet" sieve analysis; M_d is median grain diameter; S_o is Trask's sorting coefficient.
3) G is pore geometrical factor; P_d is extrapolated displacement (injection) pressure.
4) Percent clay is semi-quantitative estimate of amount of pore-filling clay based on both x-ray diffraction and thin sectio analysis; Q_v is cation exchange capacity per unit pore volume (meq/ml).

Table 2

POROSITY AND PERMEABILITY DATA FOR SELECTED ROCK CATALOG SANDSTONE SAMPLES

Sample Formation Name	Porosity and Permeability[1]		Oil End Point Relative Permeability[2]		Brine End Point Relative Permeability[2]	
	ϕ(%)	k_a (md)	k_{ro}	@ S_w(%)	k_{rw}	@ S_w(%)
"Discrete Particle" Clays						
Berea	21.2	796	1.02	28.6	0.10	64.8
Miocene "S"	22.9	1173	0.87	23.5	0.17	71.4
Paluxy	24.8	1037	1.04	20.5	0.14	68.1
Cotton Valley	14.1	150	0.96	34.0	0.23	70.1
Tar Springs	19.0	420	1.00	19.2	0.09	66.3
Average Values			0.98	25.1	0.14	68.1
"Pore-Lining" Clays						
Tuscaloosa	25.7	41	1.08	51.8	0.07	78.0
Vicksburg	18.3	7.0	1.21	25.1	0.06	60.4
Hosston*	10.9	0.82	0.67	24.7	0.25	56.0
Wilcox	13.2	1.40	0.93	37.0	0.12	65.1
Frio	26.5	58	0.92	62.4	0.13	80.0
Average Values			1.04	44.1	0.10	70.9
"Pore-Bridging" Clays						
Vicksburg	19.1	0.09	0.71	41.5	0.05	71.0
Hosston*	8.45	0.15	0.20	17.3	0.09	58.8
Wilcox	11.1	0.31	0.95	49.0	0.01	53.0
Wilcox	12.9	0.21	1.56	24.0	0.01	54.6
Average Values			1.07	38.2	0.05	59.5

* Samples show "oil-wet" properties and are excluded from average values.

1) Porosity at 1000 psig; air permeability corrected for Klinkenberg effect.[6]

2) End point relative permeability values from same sample and measured at 1000 psig. The S_w values for k_{ro} represent "immobile" brine saturation when a 30 c.p. oil is forced through the core under a pressure differential of 45 psi. The S_w values for k_{rw} represent "immobile" oil saturation (i.e., $1.0-S_o$) when brine is flowed through a core under a small pressure differential.

FIGURE Ia. - "DISCRETE PARTICLE" KAOLINITE

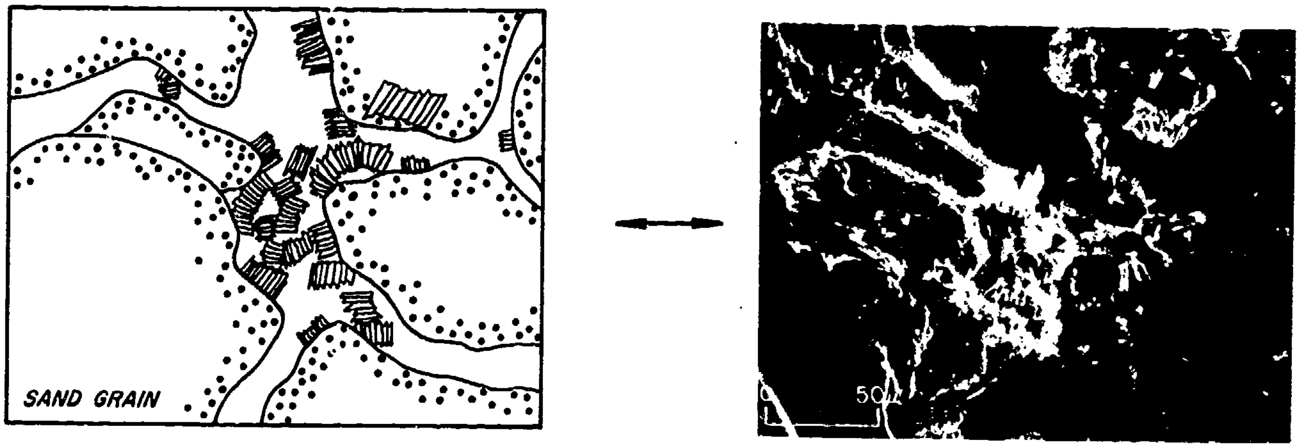

FIGURE Ib. - "PORE-LINING" CHLORITE

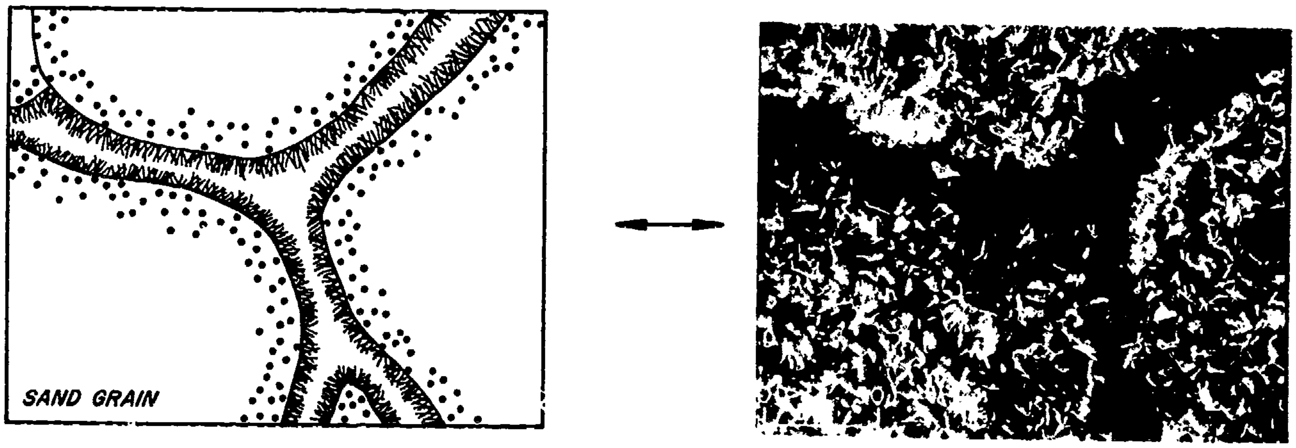

FIGURE Ic. - "PORE-BRIDGING" ILLITE

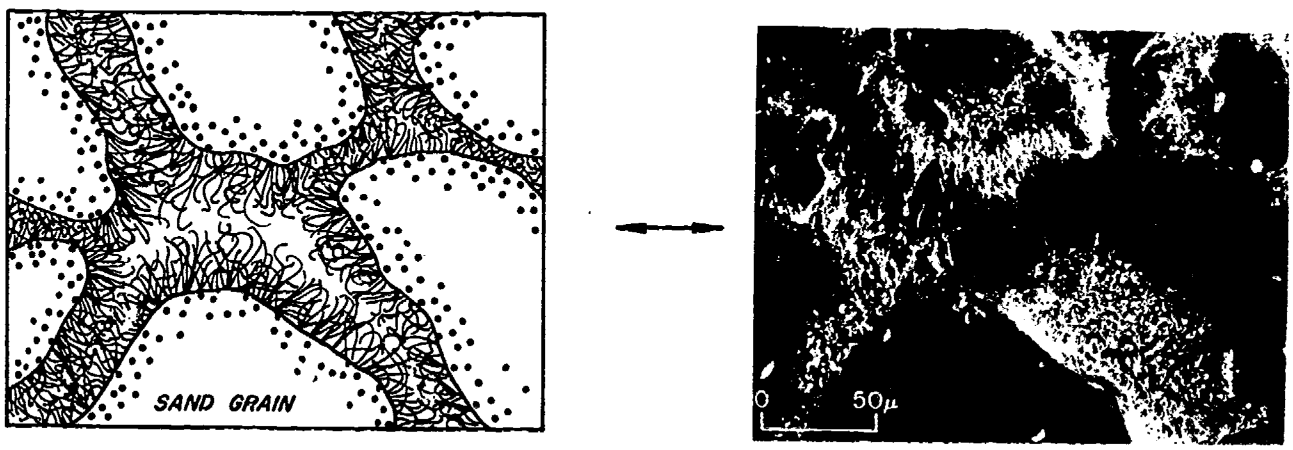

Fig. 1 - Three general types of dispersed clay in sandstone reservoir rock.

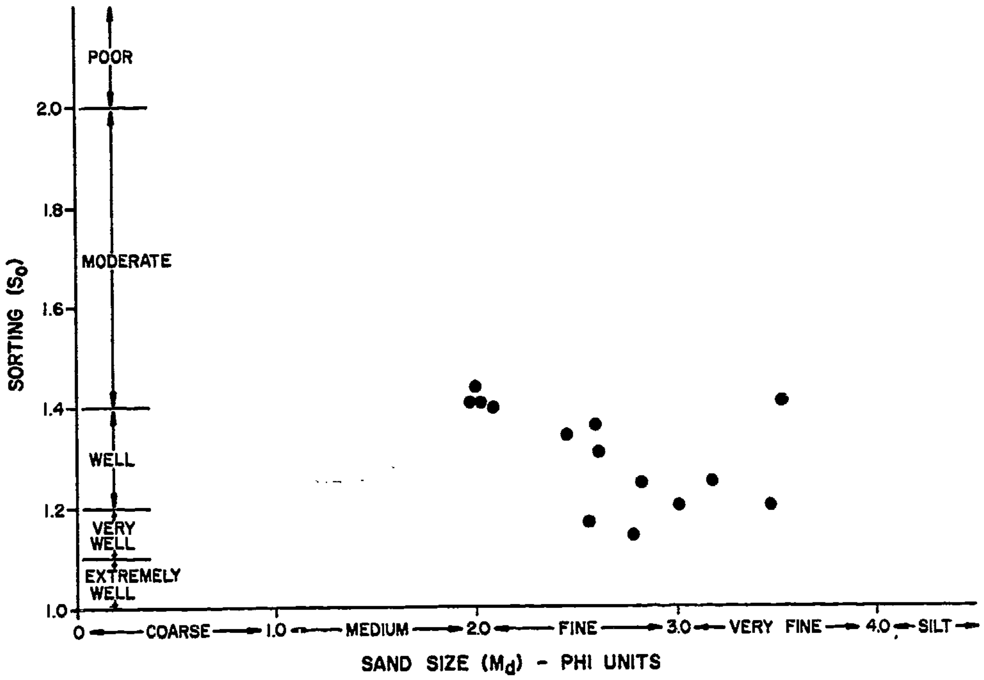

FIG. 2 - MEDIAN GRAIN SIZE (M_D) AND SORTING (S_0) PARAMETERS OF SANDSTONE SAMPLES DESCRIBED IN THIS REPORT.

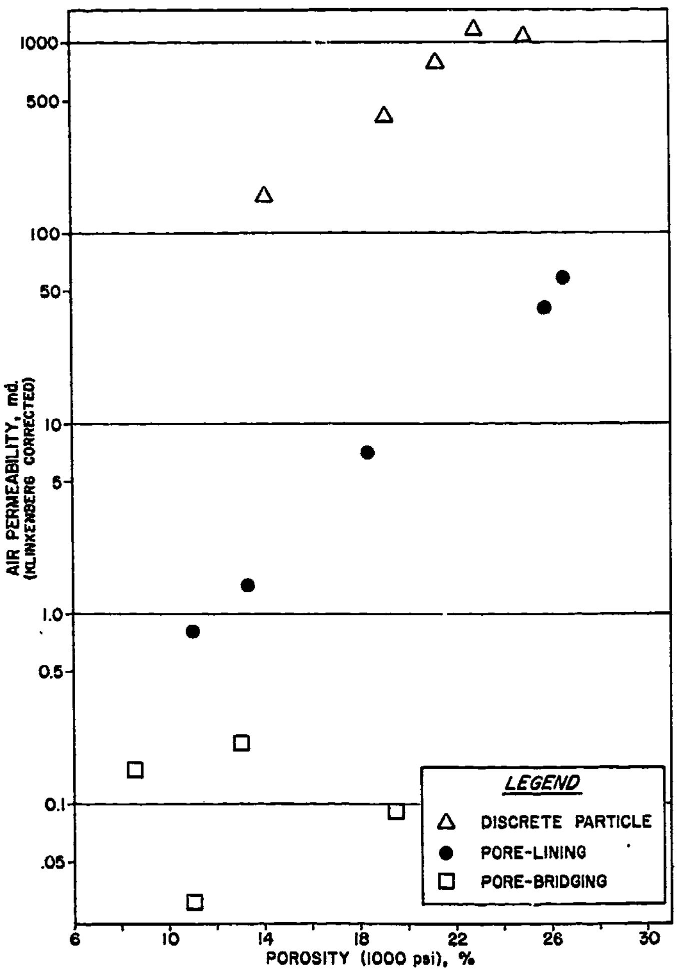

FIG. 3 - CROSS PLOT OF POROSITY AND AIR PERMEABILITY (KLINKENBERG CORRECTED [5]) FOR SELECTED SANDSTONE SAMPLES WHICH HAVE CONTRASTING DISPERSED CLAY MORPHOLOGY.

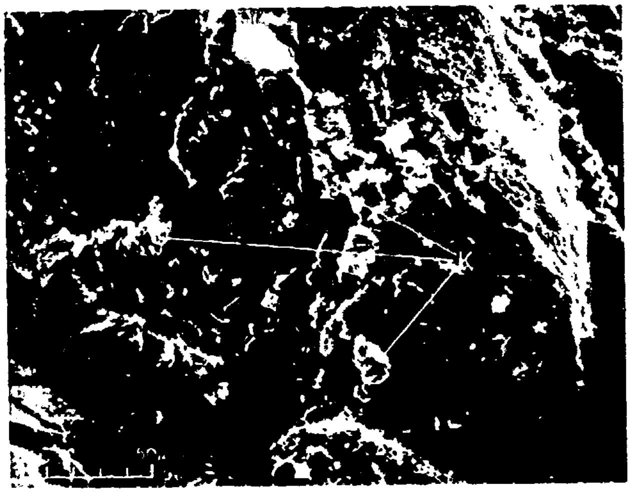

TAR SPRINGS SAND CONTAINING "DISCRETE PARTICLE" KAOLINITE (K)
ϕ = 19.0%
k_a = 420 md.

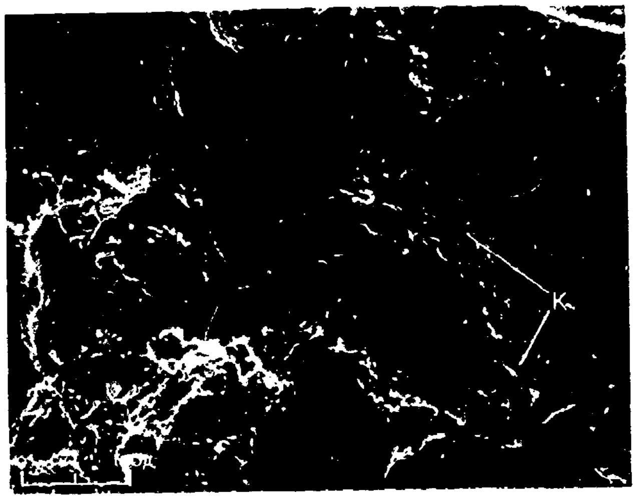

MIOCENE "S" SAND CONTAINING "DISCRETE PARTICLE" KAOLINITE (K)
ϕ = 22.9%
k_a = 1173 md.

Fig. 4 - Scanning electron microscope photomicrographs of sandstones containing "discrete particle" kaolinite.

TUSCALOOSA SAND CONTAINING "PORE-LINING" CHLORITE (C)
ϕ = 25.7%
k_a = 41 md.

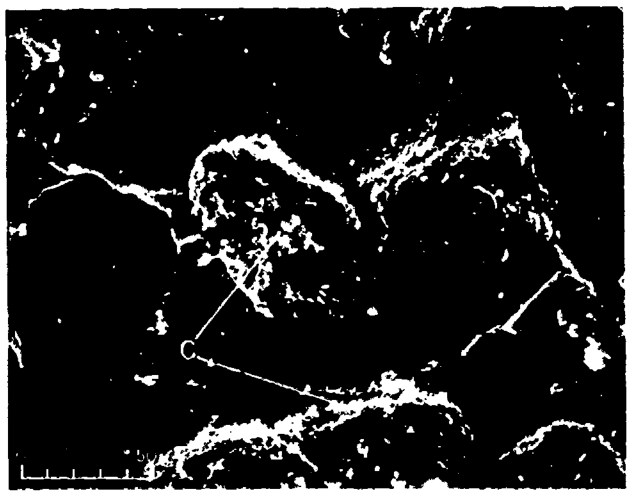

FRIO SAND CONTAINING "PORE-LINING" ILLITE AND CHLORITE (C)
ϕ = 26.5%
k_a = 58 md.

Fig. 5 - Scanning electron microscope photomicrographs of sandstones containing "pore-lining" clay minerals.

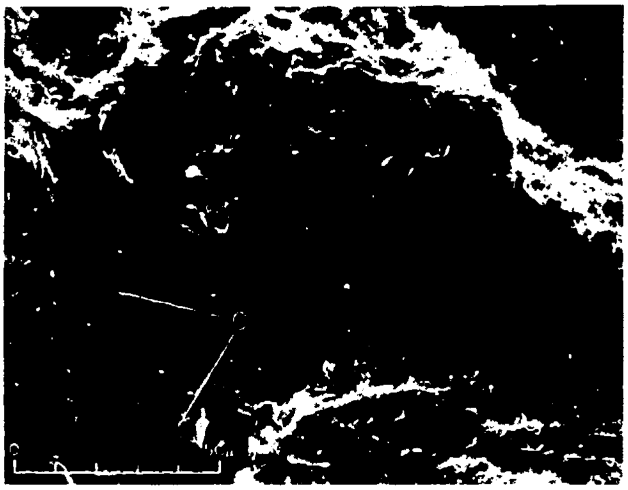

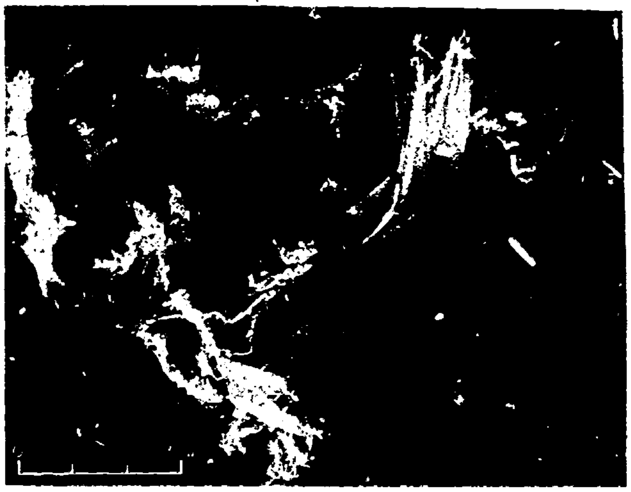

VICKSBURG SAND CONTAINING
"PORE-BRIDGING" CHLORITE (C)
ϕ = 19.1%
k_a = 0.09 md.

WILCOX SAND CONTAINING
"PORE-BRIDGING" ILLITE
ϕ = 11.1%
k_a = 0.31 md.

Fig. 6 - Scanning electron microscope photomicrographs of sandstones containing "pore-bridging" clay minerals.

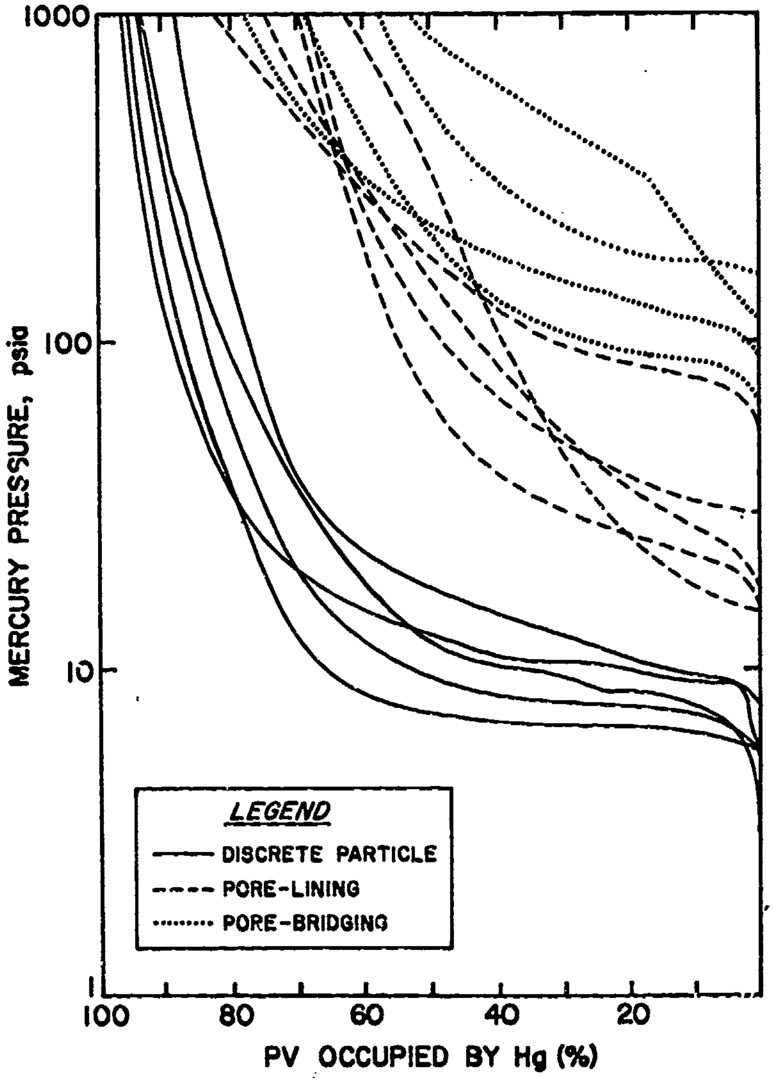

Fig. 7 - Air/mercury capillary pressure curves for selected sandstone samples which have contrasting dispersed clay morphology.